

# Direct comparison of cross-sectional scanning capacitance microscope dopant profile and vertical secondary ion-mass spectroscopy profile

Y. Huang and C. C. Williams

*Department of Physics, University of Utah, Salt Lake City, Utah 84112*

H. Smith

*Digital Equipment Corporation, Hudson, Massachusetts 01749*

(Received 8 February 1995; accepted 29 September 1995)

The scanning capacitance microscope (SCM) has been shown to be useful for quantitative 2D dopant profiling near the surface of silicon. An atomic force microscope is used to position a nanometer scale tip at a silicon surface, and local capacitance change is measured as a function of sample bias. A new feedback method has been recently demonstrated in which the magnitude of the ac bias voltage applied to the sample is adjusted to maintain a constant capacitance change as the tip is scanned across the sample surface. The applied ac bias voltage as a function of position is then input into an inversion algorithm to extract the dopant density profile. The new feedback approach allows for the use of a quasi-1D model in the inversion algorithm. Since there are no alternative 2D dopant profiling techniques which are well established at present, evaluation of the quantitative character of 2D SCM measured profiles has been a challenge. To avoid this obstacle, we have developed sample preparation methods which allow direct comparison of lateral SCM measured profiles on cleaved wafers (cross-sectional plane) with vertical secondary ion-mass spectroscopy (SIMS) profiles. The direct comparison of inverted SCM data and SIMS profiles indicates that quantitative 2D dopant profiling can be achieved by the SCM on a nanometer scale. © 1996 American Vacuum Society.

## I. INTRODUCTION

The shrinkage of semiconductor devices to the sub-micrometer level has led to the need for the direct measurement of 2D dopant profile with nanometer scale resolution. Both high sensitivity and high lateral resolution are required to achieve the goal. There are many dopant profiling techniques presently available.<sup>1</sup> The secondary ion-mass spectroscopy (SIMS) and spreading resistance profiling (SRP) are the most widely used methods for dopant profile measurements. However, they are 1D methods. Recently, several scanning probe microscopy (SPM) techniques have been applied to the 2D dopant profile measurements.<sup>2-10</sup> The scanning capacitance microscope, one of the SPMs, has shown great potential for nondestructive, direct measurement of 2D dopant profile with nanometer scale spatial resolution.<sup>11-14</sup> The successful direct measurement of dopant profile on Si from the top surface by SCM has encouraged the same measurement on cross-sectional surfaces of cleaved Si wafers. Here we report some recent progress toward direct dopant profile measurements on cross-sectional surfaces of implanted Si by SCM.

The SCM dopant profiling approach is based upon the general concepts used in 1D capacitance-voltage ( $C-V$ ) profiling.<sup>15</sup> So the carrier density, rather than the impurity density, is measured by this approach directly. Unlike the discrete dopant atom distribution, the carrier distribution is continuous over the dopant region. It has been shown, however, that when the dopant density varies moderately over a few Debye lengths (Debye length is 13 nm at a concentration of  $10^{17} \text{ cm}^{-3}$  and 0.4 nm at  $10^{20} \text{ cm}^{-3}$ ), the carrier density is a reasonably good measure of the activated dopant density.<sup>15</sup>

## II. EXPERIMENT DESCRIPTION

Our instrument is a combination of an atomic force microscope (AFM) and a SCM.<sup>12-14</sup> The block diagram of our setup is shown in Fig. 1. A tungsten tip is brought to the surface of a silicon metal-oxide-semiconductor (MOS) structure. A contact mode AFM is used to position and scan the tip over the surface of the sample. A high-sensitivity capacitance sensor developed by RCA (operating at 915 MHz) is connected to the tip to measure the capacitance between the tip and sample. The tip is grounded at low frequencies with an inductor and a 4 kHz ac bias voltage is applied to the sample.<sup>13</sup> The tip/sample capacitance change associated with the ac bias voltage (due to semiconductor depletion) is measured by the capacitance sensor and detected by lock-in amplifier. The detected signal is compared to a reference voltage and sent to a feedback controller. The feedback controller adjusts the magnitude of the ac bias voltage applied to the sample (via a voltage-controlled oscillator) as the tip is scanned over regions of varying dopant density so as to keep a constant ac capacitance change. The feedback controlled magnitude of the ac bias voltage is recorded by the computer along with the AFM topography signal as the probe is scanned across the sample. The SCM measurements can thus be directly correlated with the topographic surface profile.

## III. EXPERIMENTAL RESULTS AND DISCUSSION

The probe tips are fabricated by electrochemically etching 50  $\mu\text{m}$  tungsten wires in 2 N NaOH solution. A 15 nm radius of curvature can be achieved by this method. The sample

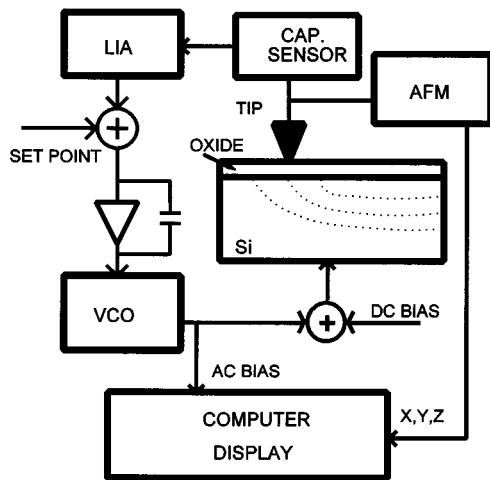


FIG. 1. Block diagram of the SCM and new feedback system.

measured by SCM in this report was a boron implanted  $p$ -type silicon wafer ( $p^+/p$ ). The Si wafer [100] was cleaved along the [010] plane to make a flat cross-sectional surface. Silicon dioxide was sputtered on the cross-sectional surface. Right after sputtering, the sample was annealed at 500 °C in  $H_2$  ambient for 30 min. This anneal process is necessary to make the oxide less porous and reduce the surface state density.<sup>16</sup> The oxide layer plays an important role in the SCM measurement. First, it is an insulating layer between the Si and the metallic tip to form a MOS structure for the capacitance measurement. Second, the surface of silicon is passivated by this oxide layer, so there is a relatively low surface state density at the interface, which is critical for the  $C-V$  measurement. We have measured  $C-V$  curves before and after the passivation. We have found that before passivation, the  $C-V$  curves could hardly reach the accumulation regime and the depletion part was stretched out. After passivation, the accumulation regime could be easily reached and the depletion part is close to that with thermal oxide. The low-temperature annealing presumably avoids redistribution of the dopant, so that we always measure the original dopant profile. Both SIMS and SRP measurements were performed on this wafer. The peak concentration on the cross-sectional surface near the top surface was measured by SRP to be  $8 \times 10^{19} \text{ cm}^{-3}$  ( $p$ -type). The topographic signal was measured simultaneously and the edge between the top surface and cross-sectional surface was used to align the SCM profile to the SIMS and SRP data.

This sample was imaged using the constant capacitance change feedback mode. The feedback loop set point was adjusted so that a very small capacitance change at each position was maintained by the feedback loop. The curve shown in Fig. 2 represents the feedback controlled magnitude of the ac bias as the tip was scanned across the cross-sectional surface near the top surface. The amplitude scale of the measured ac bias voltage can be adjusted by the set point of the integrator.

Under the feedback control, the depletion depth beneath

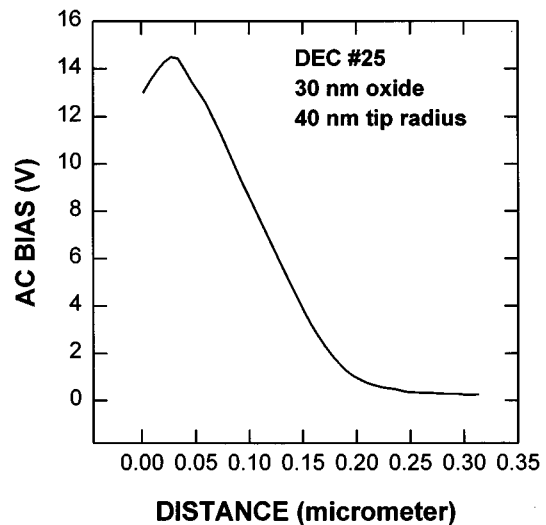


FIG. 2. The measured ac bias applied on the sample by the locked capacitance change method, as the probe moves from implanted region ( $p^+$ ) to the substrate ( $p$ ).

the tip should remain approximately the same for regions of different dopant density. If the depletion depth chosen by the set point is small compared to the tip size and oxide thickness, a quasi-1D model can be used to invert the SCM data to dopant profile. Figure 3 shows the schematic diagram of our analytical quasi-1D model used to invert the measured ac signal to the dopant density. The tip is represented by a conducting sphere in contact with an oxide on a conducting plane. The whole surface plane of the sample is divided into narrow annuli around the contact point between the tip and oxide. For each annular radius, the effective insulator capacitance is calculated by the method of images.<sup>17</sup> Once the effective gap capacitances are known for each radius, the depletion depth can be calculated for a given tip bias voltage, assuming that the depletion depth is small. The depletion capacitance in the silicon is calculated for each annular region using a simple 1D band bending model.<sup>15</sup> The total

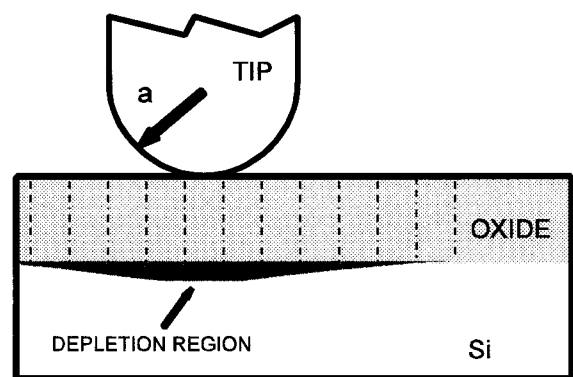


FIG. 3. Schematic diagram of the tip-sample configuration. After applying a voltage between the tip and substrate, there is a depletion region near the silicon surface.

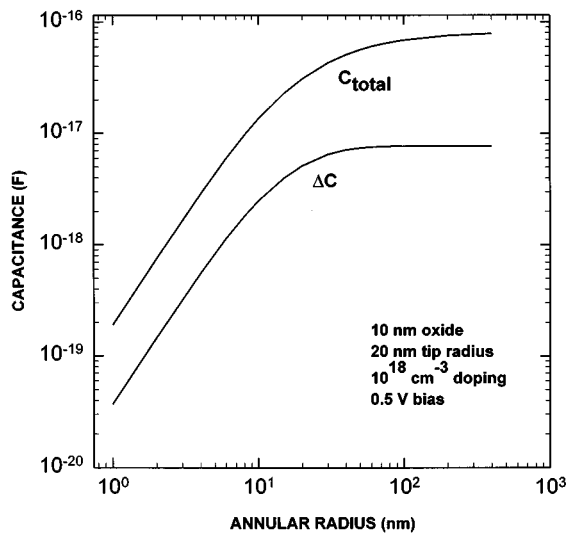


FIG. 4. The convergence of the total capacitance and the capacitance change due to applied voltage with the annular radii, showing the lateral resolution is just the tip diameter.

capacitance for each annular region is obtained by adding, in series, the effective insulator capacitance and the silicon depletion capacitance for that annular region at a given tip/sample bias voltage. The total tip/sample capacitance is obtained by integrating the capacitance contribution of each of these annular regions. The tip/sample capacitance can thus be obtained as a function of tip bias, tip radius, dielectric thickness, dopant density, and annular radius.

The insulator layer is composed of two different dielectric layers (oxide and air) with different boundary conditions (spherical between tip and air, planar between oxide and Si). It is complicated to get a precise physical model for the insulator layer. In order to get first-order results we have simplified the modeling of the insulator layer. We have assumed that the insulator layer is just the oxide layer. Based on this simplified model, we calculate both the total capacitance and the capacitance change due to the applied ac bias. Figure 4 shows these two capacitances as a function of annular radius. As shown in Fig. 4, the total capacitance between the tip and sample converges very slowly as the integration of the annular capacitance contributions is performed. This is expected since the stray capacitance is much larger than that due to fields directly below the tip. In our SCM measurements, however, only the capacitance change due to depletion under the applied ac bias is measured. It is shown that the capacitance change does converge with integrated radius much faster than the total capacitance itself. Furthermore, the capacitance change at the higher dopant densities is dominated by depletion which occurs in the silicon within one tip radii of the contact point. This indicates that the expected spatial resolution is just equal to the tip diameter. Due to the high operating frequency of the capacitance sensor, the spreading resistance in the Si substrate (in series with the tip/sample capacitance) can potentially influence the measured capacitance. However, for small tip

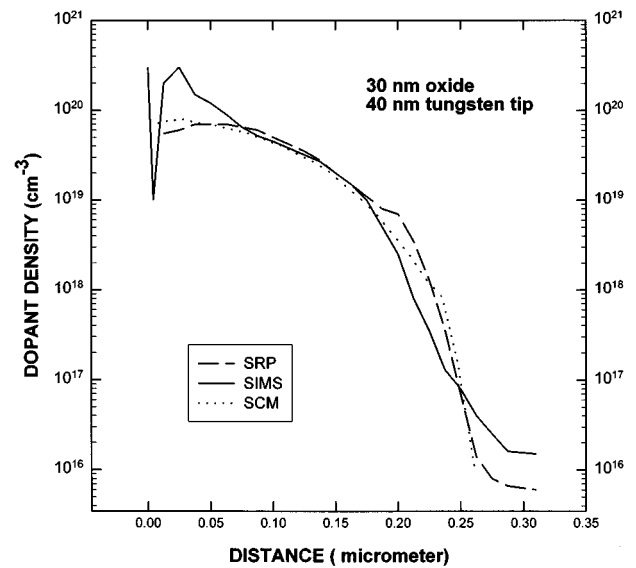


FIG. 5. The SCM profile compared with the SIMS and SRP profiles on  $p^+/p$  sample.

radii (sub 100 nm) and for dopant densities of  $10^{17} \text{ cm}^{-3}$  or greater, these spreading resistance effects can be shown to be negligible.

Only relative dopant profiles can be performed by the SCM method without the use of dopant density standards. A reference point at which the dopant density is known by an independent means is needed to find the absolute dopant profile. Here we use the highest dopant density measured by SRP as the reference point to invert the magnitude of the ac bias to absolute dopant profile. All values of the SCM profile are determined by comparison to this dopant density. A numerical inversion algorithm was written based upon our quasi-1D model to invert the SCM feedback data (magnitude of the ac bias versus lateral position) to dopant density profile.

Figure 5 shows the SCM dopant profile inverted from the measured ac voltage shown in Fig. 2. It is compared with the dopant profiles measured by SIMS and SRP. The measured values for oxide thickness (30 nm) and tip radius (40 nm) are used in the inversion calculations. When we tried to invert the data using these measured parameters, we found the inverted profile did not fit well to the SIMS and SRP results at lower dopant density. This may be due to several uncertain parameters, such as the dielectric constant of the sputtered oxide, the surface state density, and the measured oxide thickness. It is well known that sputtered oxide may be porous and can absorb some water (dielectric constant of water is 80). The dielectric constant of this layer therefore may be larger than that of pure oxide (dielectric constant is approximately 4). In order to get a good fit to the SIMS profile, we have used here a dielectric constant of 23 (75% oxide, 25% water). Using this value, the fit is reasonably good for this sample and other cross-sectional measurements. We believe that this value is physically unrealistic. The other factor in which there is some uncertainty is the oxide thickness. A

DEKTAK stylus profiler was used to perform this measurement after removing a portion of the oxide film by chemical etch. The transition from the oxide to the bare silicon was not abrupt. Therefore the accuracy of the oxide thickness measurement was not high. Conceivably, the oxide thickness could be as low as 10 nm. If this value is used in the inversion of the SCM data, a good fit can be obtained with an oxide dielectric constant of 4. Future work will include the independent measurement of the dielectric constant and improved thickness measurements, so that the ambiguity between thickness and dielectric constant will be eliminated.

Below  $10^{17} \text{ cm}^{-3}$ , the error between SCM and SIMS or SRP profiles becomes larger. At these dopant densities, the Debye length becomes comparable to the tip size, and the quasi-1D approximation breaks down. For characterization of current very large scale integrated (VLSI) structures, the important dopant density range is from  $10^{17} \text{ cm}^{-3}$  to  $10^{20} \text{ cm}^{-3}$ . The SCM appears to perform well in this range. Improvement in the inversion model may further extend the range over which the SCM can provide accurate dopant profiling.

#### IV. SUMMARY

In summary, we have performed direct dopant profile measurements on a cross-sectional surface of implanted silicon wafers by a novel SCM technique. A constant capacitance change feedback method is used to measure the ac bias applied to the sample. A quasi-1D model has been applied to invert the experimental SCM data to dopant density. The inverted SCM profile has been compared with SIMS and

SRP results. The SCM measured profile is in good agreement with both SIMS and SRP profiles over a dopant density range of  $10^{17} \text{ cm}^{-3}$  to  $10^{20} \text{ cm}^{-3}$ .

#### ACKNOWLEDGMENT

The work was supported by the Semiconductor Research Corporation.

- <sup>1</sup>R. Subrahmanyam, *J. Vac. Sci. Technol. B* **10**, 358 (1992).
- <sup>2</sup>P. Murali, H. Meier, D. W. Pohl, and H. W. M. Salemink, *Appl. Phys. Lett.* **50**, 1352 (1987).
- <sup>3</sup>S. Hosaka, S. Hosoki, K. Takata, K. Horiuchi, and N. Natsuaki, *Appl. Phys. Lett.* **53**, 487 (1988).
- <sup>4</sup>Y. Martin, D. W. Abraham, and H. K. Wickramasinghe, *Appl. Phys. Lett.* **52**, 1103 (1988).
- <sup>5</sup>D. W. Abraham, C. C. Williams, J. Slinkman, and H. K. Wickramasinghe, *J. Vac. Sci. Technol. B* **9**, 703 (1991).
- <sup>6</sup>M. B. Johnson and J.-M. Halbout, *J. Vac. Sci. Technol. B* **10**, 508 (1992).
- <sup>7</sup>S. Kordic, E. J. vanLoenen, and A. J. Walker, *J. Vac. Sci. Technol. B* **10**, 508 (1992).
- <sup>8</sup>M. B. Johnson, H. P. Meier, and H. W. M. Salemink, *Appl. Phys. Lett.* **63**, 3636 (1993).
- <sup>9</sup>C. Shafai, D. J. Thomson, M. Simard-Normandin, G. Mattiussi, and J. Scanlon, *Appl. Phys. Lett.* **64**, 342 (1994).
- <sup>10</sup>A. K. Henning, T. Hochwitz, J. Slinkman, J. Never, S. Hoffmann, and P. Kaszuba, *J. Appl. Phys.* **77**, 1888 (1995).
- <sup>11</sup>C. C. Williams, J. Slinkman, W. P. Hough, and H. K. Wickramasinghe, *Appl. Phys. Lett.* **55**, 1662 (1989).
- <sup>12</sup>K. S. Mak and C. C. Williams, *Proc. SPIE* **1556**, 90 (1992).
- <sup>13</sup>Y. Huang and C. C. Williams, *J. Vac. Sci. Technol. B* **12**, 369 (1994).
- <sup>14</sup>Y. Huang, C. C. Williams, and J. Slinkman, *Appl. Phys. Lett.* **66**, 344 (1995).
- <sup>15</sup>E. H. Nicollian and J. R. Brews, *MOS Physics and Technology* (Wiley, New York, 1982).
- <sup>16</sup>S. Wolf and R. N. Tauber, *Silicon Processing for the VLSI Era* (Lattice, Sunset Beach, CA, 1986), Vol. 1.
- <sup>17</sup>J. D. Jackson, *Classical Electrodynamics* (Wiley, New York, 1975).